Zdzisław WŁODARSKI[1], Jadwiga WŁODARSKA[2]

Maritime University of Szczecin (1), West Pomeranian University of Technology (2)

Reduced equations of magnetic hysteresis generated by quasi-elastic rotations of domains

Abstract. *Magnetization processes are described by quasi-elastic rotations of domains. Thanks to this, basic curves of magnetic hysteresis are approximated by the reduced equation. Its extended form takes into account dependence of magnetization on frequency and temperature.*

Streszczenie. *Procesy magnesowania opisano poprzez quasi-sprężyste obroty domen. Dzięki temu podstawowe krzywe histerezy magnetycznej aproksymowano równaniem zredukowanym. Jego rozszerzona postać uwzględnia zależność namagnesowania od częstości i temperatury.* (**Procesy magnesowania opisane poprzez quasi-sprężyste obroty domen**)

Keywords: magnetization, hysteresis, temperature.
Słowa kluczowe: namagnesowanie, histereza, temperatura.

Introduction

Mathematical description of magnetic hysteresis is necessary in many problems. Magnetic materials are used in transformers, motors, generators and other devices, while hysteresis effects occur in many branches of physics, medicine, or economy. Analysis of magnetic phenomena proceeds in two stages. Quantum theory explains the spontaneous formation of domains, within which all atomic magnetic moments are arranged unidirectional, and determines general anhysteretic relation between magnetization and field in the form of Brillouin function [1]. Then, different models explain hysteresis effects. The most known of them are the Jiles-Atherton model [2] based on physical assumptions and Preisach-type models [3] using triangular diagrams of hysteresis. Simpler models approximate hysteresis curves by functions producing their S-shaped equivalents [4,5]. All these models use several fitting parameters and in general lead to numerical solutions of related electrical circuits. Presented description enables analytical determination of basic hysteresis curves and circuit characteristics without referring to specific material parameters. Extended forms of the model describe frequency and temperature effects.
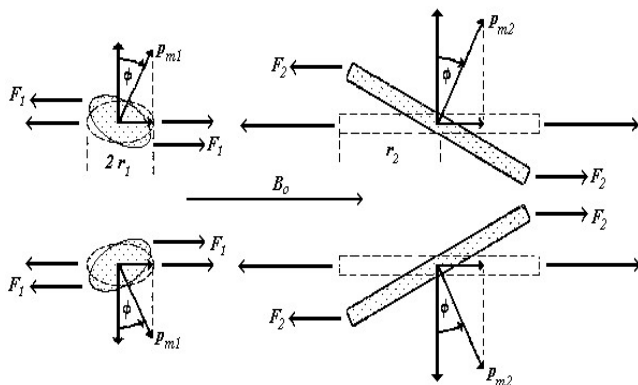

Fig.1. Simplified model of reversible and irreversible rotations

Initial magnetization curve

Magnetic material consists of randomly oriented domains. In an external field H the domains aligned to field grow at the expense of others and turn in the direction of field, until all of them are aligned to it and saturation magnetization M_s is achieved. The real set of domains we replace by an idealized system of two groups of domains, and the process of magnetization will be reduced to rotations. The first group consists of N_1 domains with magnetic moments p_{m1}, the second group consists of N_2

domains with magnetic moments p_{m2}. Both groups are arranged into pairs perpendicular to magnetic induction $B_0 = \mu_0 H$, like in Fig.1.

The field turns each domain until the moment of magnetic forces is compensated by the moment of internal elastic forces. For the first group we assume constant internal forces F_1, which leads to relation

$$(1) \qquad p_{m1}\mu_0 H \cos(\phi) = 2\,r_1\,F_1\,\sin(\phi)$$

Hence we get $\phi = atan(H/a)$, where $a = 2r_1F_1/(\mu_0 p_{m1})$. The considered pair of domains generates in the field direction the resultant moment $p_H = 2p_{m1}sin(atan(H/a))$, and all $N_1/2$ pairs of these domains give magnetic moment

$$(2) \qquad M_1 = M_a\,S\!\left(\frac{H}{a}\right)$$

where $M_a = N_1 p_{m1}$, and

$$(3) \qquad S(x) = \sin(atan(x)) = \frac{x}{\sqrt{1+x^2}}$$

For the second group we assume internal forces F_2 decreasing with the rise of field due to weakening ties with neighboring elements. We describe this effect by the saturation function (3) using variable $x = H/b$

$$(4) \qquad p_{m2}\mu_0 H \cos(\phi) = 2\,r_2\,\frac{F_0}{S(|H|/b)}\sin(\phi)$$

where $b = 4r_2 F_0/(\mu_0 p_{m2})$. If $M_b = N_2 p_{m2}$, the resultant magnetization of all $N_2/2$ pairs of these domains is

$$(5) \qquad M_2 = M_b\,S\!\left[S\!\left(\frac{|H|}{b}\right)\frac{2H}{b}\right]$$

Thus, the total initial magnetization will be

$$(6) \qquad M(H) = M_a\,S\!\left(\frac{H}{a}\right) + M_b\,S\!\left[S\!\left(\frac{|H|}{b}\right)\frac{2H}{b}\right]$$

where $M_a + M_b = M_s$, and a, b determine the rate of approach to saturation for reversible (2) and irreversible (5) processes. This curve is presented by the solid line in Fig. 2.

Quasi-static loops

If magnetic field changes cyclically from the maximum value H_m to minimum value $-H_m$, the corresponding changes in orientation of domains from the state achieved in maximum point $(H_m, M(H_m))$ run initially slower (dashed-

dotted line in Fig. 2) than in initial process, leaving at $H = 0$ remanent magnetization M_r. It is reduced to zero when the field assumes negative value $-H_c$. Then, the sample magnetizes to the minimum value $-M_m = M(-H_m)$ and returns to the highest point along a lower, symmetrical branch of the loop (dotted line in Fig.2).
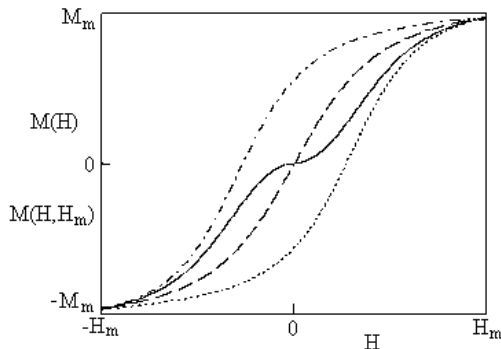

Fig.2. Initial curve, anhysteretic curve, and symmetrical loop

Suppose that changes of magnetization from the highest point of small loops run like changes from the initial state. It means that the expression $(H_m - H)$ varies linear in the first component of (6) and quadratic in the second component. This assumption generates an upper branch of hysteresis loop

(7)
$$M(H, H_m) = M_a S\left(\frac{H_m - (H_m - H)}{a}\right) + M_b S\left[S\left(\frac{H_m}{b}\right)\frac{2H_m^2 - (H_m - H)^2}{b H_m}\right]$$

The lower branch is determined by the central symmetry condition $M'(H, H_m) = -M(-H, H_m)$.

Relation (7) describes small hysteresis loops of width H_m. When magnetization approaches saturation, the width of quasi-static loops approaches certain maximum value. Assuming that it is equal to b, we describe this change by the saturation function $S(H_m/b)$, and write (7) as the sum of central anhysteretic curve and deviation from it

(8)
$$M(H, H_m) = M_a S\left(\frac{H}{a}\right) +$$
$$M_b S\left\{S\left(\frac{H_m}{b}\right)\left[\frac{2H}{b} \pm S\left(\frac{H_m}{b}\right)\frac{2H_m^2 - (H_m - H)^2 - 2H_m H}{H_m^2}\right]\right\}$$

where the signs $\pm$ specify upper or lower branch of the loop.

Reduced form of quasi-static loops

For not too high field amplitudes, the first component of (8) may be neglected, because usually $a \gg b$. By introducing normalized expressions

$x = H/b$, $y = M/M_b$, $x_m = H_m/b$, $y_m = M_m/M_b$

we eliminate from (8) material parameters and get the reduced equation of symmetrical loops and related curves

(9) $\quad y(x, x_m, \delta) = S\left\{S(x_m)\left[2x + \delta S(x_m)\left(1 - \frac{x^2}{x_m^2}\right)\right]\right\}$

where $\delta = \pm1, 0$. Central ($\delta = 0$) and initial curve (joining the tips of symmetrical loops, $x_m = |x|$) are given by

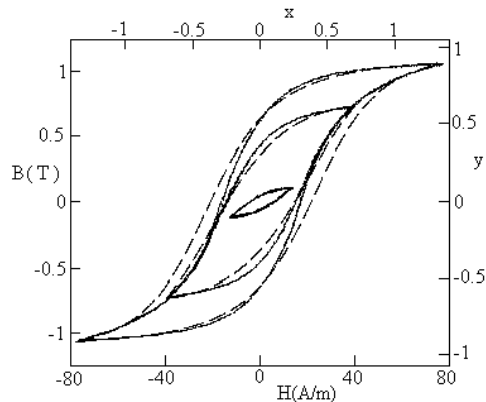(10) $\quad y_c(x, x_m) = S(S(x_m)2x)$

(11) $\quad y_i(x) = S(S(|x|)2x)$

Fig.3. Measured [6] and model (dashed) hysteresis loops of steel (cut angle $= \pi/4$, $M_b = 0.93$ MA/m , $b = 57$ A/m)

Hysteresis loops may be also generated by cyclic changes of voltage and related to it magnetization. In this model we avoid related to this numerical calculations, because (9)-(11) may be written in inverse form, directly determining the dependence of reduced field on reduced magnetization

(12) $\quad x_i(y) = y\sqrt{\dfrac{y^2 + \sqrt{16y^2 - 15y^4}}{8y^2(1 - y^2)}}$

(13) $\quad x_c(y, y_m) = \dfrac{y}{2\sqrt{1 - y^2}}\sqrt{1 + \dfrac{1}{x_i(y_m)^2}}$

(14)
$$x(y, y_m, \delta) = \dfrac{x_i(y_m)\sqrt{1 + x_i(y_m)^2}}{\delta} \times$$
$$\times \left[1 - \sqrt{1 + \dfrac{\delta^2}{1 + x_i(y_m)^2} - \dfrac{\delta y}{\sqrt{1 - y^2}\, x_i(y_m)^2}}\right]$$

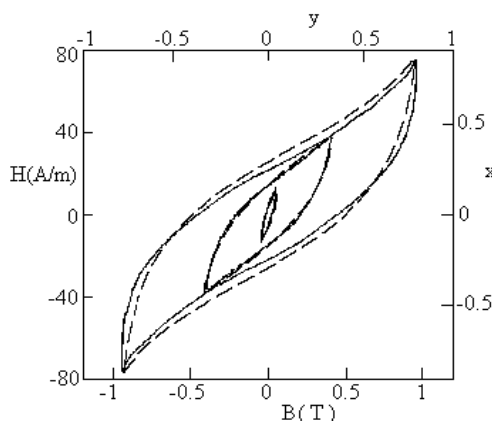Experimental [6] and model (9), (14) reduced hysteresis loops of laminated steel are compared in Figs.3, 4.

Fig.4. Inverse measured [6] and model (dashed) hysteresis loops of steel (cut angle $= \pi/2$, $M_b = 0.993$ MA/m, $b = 88.4$ A/m)

Time dependence of reduced field and magnetization

Let us consider a series circuit consisting of the source of supply of low angular velocity $\omega = 2\pi/T$, the ohmic resistance R and N turns of wire wound on a closed toroidal ferromagnetic core of length l and cross-section area A. For

sinusoidal current supply $I(t) = I_m sin(\omega t)$ we have

$$(15) \quad x(t) = \frac{H(t)}{b} = \frac{N I_m}{l\,b} \sin(\omega t) = x_m \sin(\omega t)$$

and for sinusoidal voltage supply $U(t) = U_m sin(\omega t + \pi/2)$

$$(16) \quad y(t) = \frac{M(t)}{M_b} = \frac{U_m}{\mu_0 A N \omega M_b} \sin(\omega t) = y_m \sin(\omega t)$$

where I_m, U_m are the amplitudes of current and voltage. in these cases equations (9), (14) change into analytical functions of time (with $\delta = -sign[\cos(\omega t)]$), and the numerical analysis of circuits becomes redundant.

Time dependence form of (9) for y at sinusoidal supply of x is shown in Fig.5, while the time dependence form of (14) for x at sinusoidal supply of y is plotted in Fig.6. In circuits with ferromagnetic cores these diagrams correspond to the time dependence of magnetic induction at sinusoidal supply of current, and time dependence of field and current at sinusoidal supply of voltage. Reduced magnetization $y(t)$ in Fig.6 is delayed in phase by $\pi/2$ relative to $u(t)= U(t)/U_m)$. The dashed curve corresponds to the dynamic loop (18).
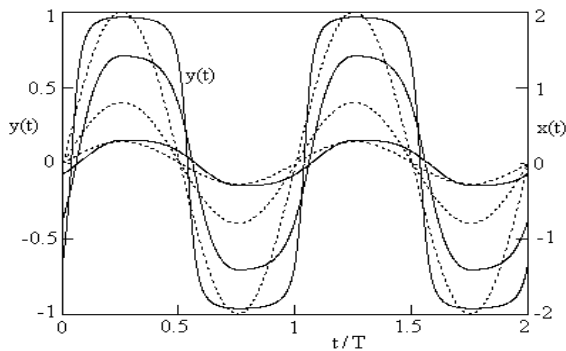

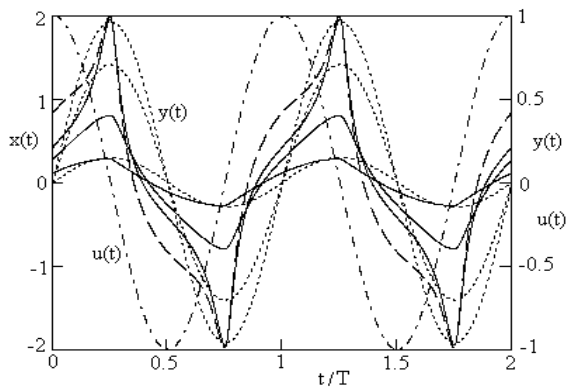Fig.5. Time dependence of y (solid) at sinusoidal supply of x (dotted)

Fig.6. Time dependence of x (solid) at sinusoidal supply of y (dotted); dashed–dependence for a dynamic loop ($\tau f = 0.16$)

Reversal curves

If a steady supply producing field x_s is added to the sinusoidal supply generating loops of amplitude x_m, then the hysteresis loop is limited by two extreme fields $x_0 = x_m + x_s$ and $x_1 = x_m - x_s$. The upper branch of the loop is given by (9) with x_m replaced by x_0. It abruptly ends at field x_1 and related magnetization $y(x_1, x_0, \delta)$ resulting from (9). From this point magnetization returns to the highest point $(x_0, y_i(x_0))$ in the same way as symmetrical branches (8) from their extreme points.

Sometimes, the curve returning from the reversal point does not achieve the top of symmetrical loop, but ends at

the lower point $(x_2, y_1(x_2, x_0, x_1))$. The return from this second order reversal point to the first reversal point will be approximated in the same way as previously. This method may be applied to further similar processes ending at the successive reversal fields $x_3, x_4, \ldots , x_n$, which leads to relation

$$(17)$$

$$y_n(x, x_0, x_1, \ldots x_n) = S\left\{\frac{S(x_0)}{1} \times\right.$$

$$\left. \left[2x \pm S(x_0)\, \frac{2x_0^2 - (x_0 - x_1)^2 + (x_1 - x_2)^2 \ldots \pm (x_n - x)^2 - 2x_0 x}{x_0^2}\right]\right\}$$
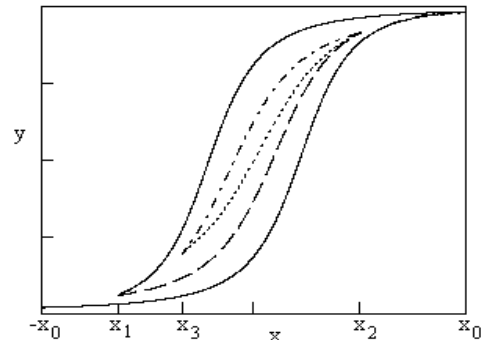
Some model reversal curves are plotted in Fig. 7.

Fig.7. Reversal curves (17)

Dynamic loops

For not too high amplitude and frequency, the reduced equations may be extended to dynamic loops characterized by the increase of the width of loops with the rise of frequency f and magnetization amplitude [5]. This effect may be achieved by the addition of a simple expression to (14)

$$(18) \quad x(y, y_m, \delta, f) = x(y, y_m, \delta) - \delta \sqrt{\tau f \left(y_m^2 - y^2\right)}$$

For soft ferromagnetic materials: $\tau \sim \mu_0 \gamma d^2 M_b/b$, where d, γ – thickness and conductivity of sheets. Comparison of model and measured dynamic loops of transformer steel is shown in Fig.8. For transition to reduced curves were applied parameters $M_b = 0.796$ MA/m, $b = 179$ A/m, $\tau = 0.0016$.
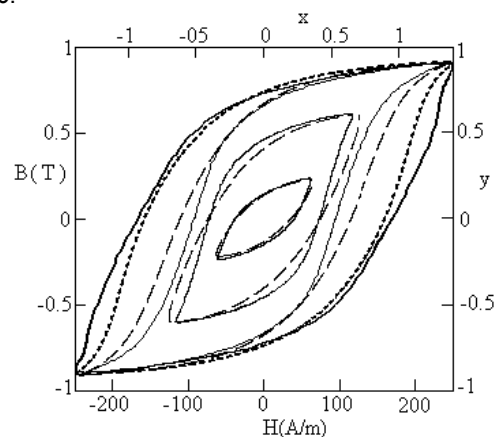

Fig.8. Measured (solid) and model (dashed) dynamic loops of steel (thinner curves – 50 Hz, thicker curves – 200 Hz)

The area (19) inside the loop determines reduced energy loss w in unit volume of a core per one cycle of hysteresis. Real losses are $W = \mu_0 M_b b w$.

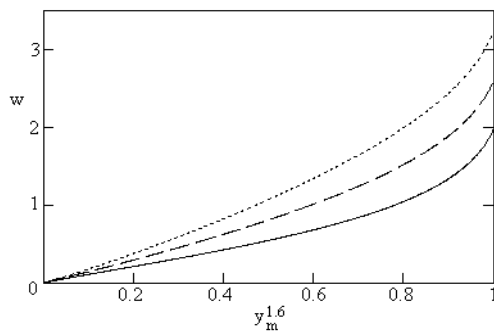$$(19) \qquad w = 2 \int_{y_m}^{-y_m} x\big(y, y_m, |\delta|, f\big)\,dy$$

Fig.9. Reduced hysteresis loss (solid – $\tau f = 0$, dashed - $\tau f = 0.04$, dotted - $\tau f = 0.16$)

Dependence of magnetization on temperature

Reduced equations can be extended to larger loops by addition of reversible component $M_a S(H/a)$. Suppose, that parameters M_a, a, M_b change with the relative temperature $\vartheta = T/T_c$ (T_c - Curie point) like function $F(\vartheta)=sqrt(1-\vartheta^n)$, while parameter b varies like $F(\vartheta)/\vartheta$. These assumptions are simpler than relations used in [7], [8], [9] and enable more accurate approximation of experimental magnetization curves (Fig.10) in a wide range of temperature.
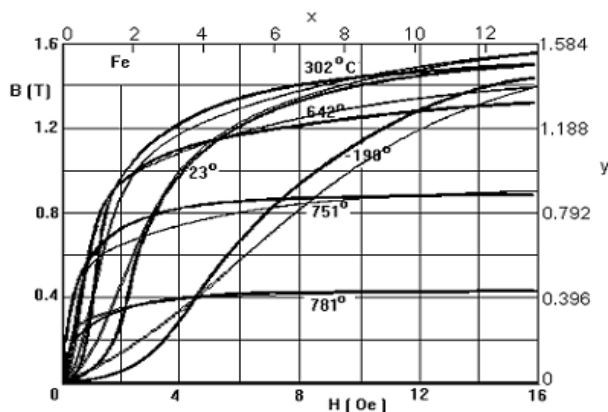

Fig.10. Temperature dependence of initial magnetization (thicker – measured [10], thinner – model (20))

Let use introduce to (9) the reversible component and assumed dependencies of model parameters on temperature. In this way we get relations

$$(20) \qquad \frac{y_i(x,\vartheta)}{F(\vartheta)} = S\left[S\left(\frac{|x\vartheta|}{F(\vartheta)}\right) \frac{2x\vartheta}{F(\vartheta)} \right] + \alpha\, S\left(\frac{\beta x}{F(\vartheta)}\right)$$

$$(21) \qquad \frac{y_c(x,x_m,\vartheta)}{F(\vartheta)} = S\left[S\left(\frac{x_m\vartheta}{F(\vartheta)}\right) \frac{2x\vartheta}{F(\vartheta)} \right] + \alpha\, S\left(\frac{\beta x}{F(\vartheta)}\right)$$

$$(22) \qquad \frac{y(x,x_m,\delta,\vartheta,f)}{F(\vartheta)} =$$
$$S\left[\begin{array}{l} S\left(\dfrac{x_m\vartheta}{F(\vartheta)}\right) \dfrac{2x\vartheta}{F(\vartheta)} + \Delta(\delta,f,\vartheta) \\[2mm] \times \left(\dfrac{x_m\vartheta}{F(\vartheta)}\right)^2 \left(1 - \dfrac{x^2}{x_m^2}\right) \end{array} \right] + \alpha\, S\left(\dfrac{\beta x}{F(\vartheta)}\right)$$

where

$$(23\ a,b,c) \qquad F(\vartheta) = \sqrt{1 - \vartheta^n}\ , \quad \alpha = M_a/M_b\ , \quad \beta = b/a$$

$$(24) \qquad \Delta(\delta,f,\vartheta) = \delta\left(1 + \sqrt{\tau f\big(y_i(x_m,\vartheta)^2 - y_c(x,x_m,\vartheta)^2 \big)} \right)$$
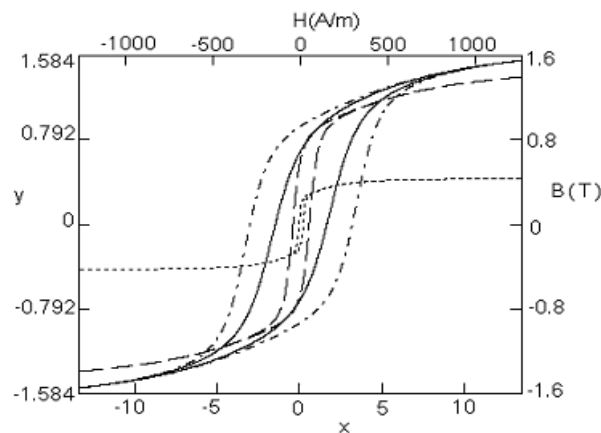

Fig.11. Computed quasi-static and dynamic loops (22) of iron (solid - $T_1 = 23^oC$; dashed - $T_3 = 642^oC$, dotted – $T_5 = 781^oC$, dashed-dotted - $T_1 = 23^oC$, $\tau f = 1$)

The results for parameters
$M_b = 0.804\ MA/m$, $b = 94.8\ A/m$, $M_a = 0.557\ MA/m$,
$a = 1005\ A/m$, $n = 9.97$, $T_c = 1061\ K$,
optimized for measured curves [10], are shown in Figs.10, 11.

Conclusion

Presented model properly describes basic curves of magnetic hysteresis. Reduced form of equations enables their application to other similarly running processes.

REFERENCES
[1] Bertotti G., Mayergoyz I.D., *The Science of Hysteresis*, Elsevier, Amsterdam, 2006.
[2] Jiles D., *Introduction to Magnetism and Magnetic Materials*, Chapman and Hall, 1998, London.
[3] Mayergoyz I.D., *Mathematical models of hysteresis*, Elsevier, Amsterdam, 2003.
[4] Takács J., *Mathematics of Hysteretic Phenomena*, Wiley-VCH Verlag, 2003, Weinheim.
[5] Włodarski Z., Analytical description of magnetization curves, *Phys. B* 373 (2006), 323-327.
[6] Finocchio G., Carpentieri M., Cardelli E., Azzerboni B., Analytical solution of Everett integral using Lorentzian Preisach function approximation, *Journal of Magnetism and Magn. Materials,* 300, 2006, 451-470.
[7] Włodarski Z., Włodarska J., Analytical approximation of the dependence of magnetic material properties on temperature, *COMPEL,* Vol.17, No. 1/2/3, 1998, 402 – 406.
[8] Zhang P., Zuo F., Urban F.K., Khabari A., Griffith P., Hosseini-Tehrani A., Irreversible magnetization in nickel nanoparticles, *Journ. of Magnetism and Magn. Materials*, 225 (2001), 337–345.
[9] Ladjimi A., Mekideche M.R., Modeling of thermal effects on magnetic hysteresis using the Jiles-Atherton model, *Przegląd Elektrotechniczny,* R.88, 4a/2012, 253 -256.
[10] Bozorth R. M., *Ferromagnetism,* IEEE Press, 1993.

Authors: *Zdzisław Włodarski, Maritime University of Szczecin; Jadwiga Włodarska, West Pomeranian University of Technology, E-mail:* wlodars@vp.pl